Photorefractive Gunn effect

Luis L. Bonilla, Manuel Kindelan, and Pedro J. Hernando
Universidad Carlos III de Madrid, Escuela Politécnica Superior, 28911 Leganés, Spain
(Received 23 January 1998)

We present and numerically solve a model of the photorefractive Gunn effect. We find that high-field domains can be triggered by phase-locked interference fringes, as has been recently predicted on the basis of linear stability considerations. Since the Gunn effect is intrinsically nonlinear, we find that such considerations give at best order-of-magnitude estimations of the parameters critical to the photorefractive Gunn effect. The response of the system is much more complex, including multiple wave shedding from the injecting contact, wave suppression, and chaos with spatial structure. [S0163-1829(98)06335-8]

I. INTRODUCTION

Segev, Collings, and Abraham[1] (SCA) proposed an interesting mechanism for producing Gunn domains by means of a photorefractive parametric excitation. It occurs when two optical waves of slightly different frequencies are incident upon a biased semiconductor crystal doped with deep impurity centers. The authors conjecture that the resulting traveling interference pattern excites multiple high-field Gunn domains that move phase locked with the interference fringes. Recently, Subacius *et al.*[2] proposed an efficient way of creating simultaneously a number of quasilocalized high-field Gunn domains through hot carrier transport in spatially modulated and nonuniformly heated electron-hole plasma, and presented some numerical results and preliminary experimental confirmation.

In this paper we present a consistent model of the photorefractive Gunn effect and carry out numerical simulations to understand the dynamics of the system. We find that high-field domains can indeed be triggered by phase-locked interference fringes, as suggested by SCA. However, the response of the system can be very complex, and it is not possible to use a simplified version of Kroemer's NL criterion, as suggested by SCA, to predict the number of high-field Gunn domains traveling through the sample. Indeed, our results indicate that with appropriate values of the parameters of the system the response becomes chaotic and this is, therefore, another example of driven (sinusoidal interference pattern of intensity I) chaos.

II. MODEL EQUATIONS

The following equations describe the photorefractive Gunn effect:

$$\frac{\partial N_D^i}{\partial t} = SI(N_D - N_D^i) - \gamma n N_D^i, \tag{1}$$

$$\frac{\partial n}{\partial t} - \frac{\partial N_D^i}{\partial t} = \frac{1}{q}\frac{\partial J}{\partial z}, \tag{2}$$

$$\frac{\partial E}{\partial z} = -\frac{q}{\varepsilon_s}(n + N_A - N_D^i), \tag{3}$$

where Eqs. (1) and (2) are the continuity equations for ionized donors and for electrons, respectively, and Eq. (3) is Poisson's law. In these equations, z is the space variable in the direction of current flow, t is the time, $N_D^i(z,t)$ represents the number density of ionized donors, N_D the total donor density, $I(z,t)$ the incident light intensity, S the photoionization cross section, γ the recombination rate, $n(z,t)$ the electron number density, $-q$ the electron charge, $J(z,t)$ the current density, $E(z,t)$ the space-charge field inside the crystal, N_A the density of negatively charged acceptors, and ε_s the low-frequency dielectric constant.

The light intensity $I(z,t)$ is given by

$$I(z,t) = I_0[1 + m\ \cos(Kz + \Omega t)], \tag{4}$$

which, as decribed in Ref. 1, is the intensity of the moving interference pattern formed when two quasimonochromatic plane waves of slightly different frequencies, ω and $\omega + \Omega$ $(\Omega \ll \omega)$, and slightly different angles of incidence illuminate a bulk semiconductor crystal. In Eq. (4), $K = 2\pi/\Lambda$ is the interference wave number, m the modulation depth of the interference grating, and I_0 the total average intensity.

Following Sze[3] [Eq. (28) in Chap. 11], the current density J includes drift and diffusion terms,

$$J = qnv(E) + q\frac{\partial[D(E)n]}{\partial z}, \tag{5}$$

which is the standard form of the drift-diffusion current density[4,5] where $v(E)$ is the electron drift velocity and $D(E)$ the diffusion coefficient. The drift velocity of the electrons is a known function of the electric field exhibiting negative differential resistance. In the following analysis we use a saturating drift velocity function given by,

$$v(E) = v_s\left[1 + \frac{E/E_s - 1}{1 + A(E/E_s)^\beta}\right], \tag{6}$$

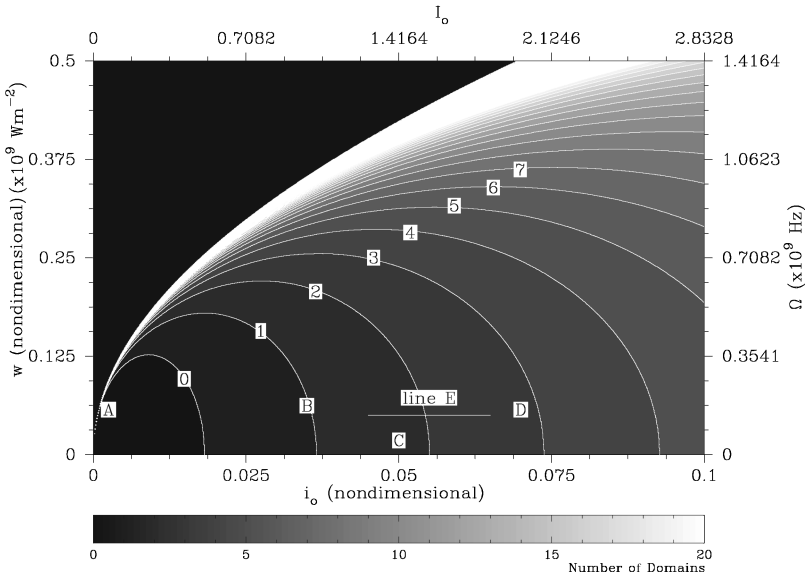

FIG. 1. Level curves of intensity versus driving frequency for different integer values of N_0 in Eq. (1). Numerical simulations have been performed for points labeled A, B, C, and D, with dimensionless values of intensity and frecuency (i_0,w): $A=(0.0025,0.05)$, $B=(0.035,0.055)$, $C=(0.05,0.0109)$, $D=(0.07,0.05)$. The Fourier spectrum of the current will be displayed later in Fig. 3 for the points on the horizontal line E.

where v_s is the saturation drift velocity, E_s the saturation field, and A and β dimensionless constants that depend explicitly on the mobility of the material ($\mu=v_s/E_s$).

Differentiating the Poisson equation (3) with respect to time, inserting the result in the continuity equation for electrons (2), and integrating with respect to space, results in $\varepsilon_s \partial E/\partial t + J = J_{\text{total}}$. Here the constant of integration, J_{total}, is the total current density. Introducing the electron current density given by Eq. (5) in the previous equation leads to Ampère's equation,

$$J_{\text{total}} = qnv(E) + q\frac{\partial[D(E)n]}{\partial z} + \varepsilon_s \frac{\partial E}{\partial t}. \tag{7}$$

Notice that in Eq. (6) of Ref. 1 the current density erroneously includes the displacement term, and this leads to an incorrect Ampère's equation in which the displacement current drops out.

In addition to these equations, the electric field distribution must satisfy the *reverse bias* condition for a given applied voltage V,

$$\int_0^L E\,dz = V. \tag{8}$$

Thus, to model the photorefractive Gunn effect we use the correct form of Ampère's law (7), the continuity equation for ionized donors (1), Poisson's law (3), the bias condition (8), and appropriate initial and boundary conditions. Solution of these equations using the known functions for the light intensity (4) and drift velocity (6) provide the four unknowns, $N_D^i(z,t)$, $n(z,t)$, $E(z,t)$, and $J_{\text{total}}(t)$.

It should be emphasized that boundary conditions play an essential role in the existence of the Gunn effect. Although it can be debated which are the correct conditions to apply in order to simulate a particular experiment, periodic boundary conditions, as used in Ref. 1, should be avoided: they yield a total current density that is constant in time when a dc voltage bias is imposed. In fact, integrating Ampère's law we find $J_{\text{total}} = L^{-1}[\varepsilon_s dV/dt + \int_0^L J\,dx]$. Then imposing periodic boundary conditions and a dc voltage bias we find that $dJ_{\text{total}}/dt = (c/L)\int_0^L (\partial J/\partial x)dx = 0$ (provided we have a domain moving at constant speed c; note that with physically reasonable boundary conditions, the domain cannot move at constant speed as it arrives at a realistic contact, e.g., Ohmic). Since the Gunn effect refers to time-dependent oscillations of the current under dc voltage bias, one should not use periodic boundary conditions when discussing it.

The most important boundary condition in a study of the Gunn effect in long samples is that for the injecting contact. In fact, the formation of Gunn domains is due to a periodic destabilization of the boundary layer attached to such contact during the oscillations.[4,5] During the formation of a new wave at the injecting boundary, the displacement current plays a crucial role and cannot be neglected. Thus, we use an Ohmic condition at the injecting contact, $E=\rho J_{\text{total}}$,[5–8] and $\partial E/\partial z = 0$ at the receiving contact (which is thus passive and integration time is saved). When ρ is such that $E/(\rho q N_A)$ intersects $v(E)$ on its decreasing branch, the Gunn effect is found for $m=0$ and appropriate values of the bias V.[4,5]

In order to solve numerically our model equations, we will first write them in nondimensional form. Let us redefine our variables in dimensionless form as follows:

$$y = \frac{1}{L}z, \quad s = \frac{v_s}{L}t, \quad F = \frac{E}{E_s},$$

$$j = \frac{J_{\text{total}}}{v_s q N_A}, \quad p = \frac{N_D^i}{N_A}, \quad \eta = \frac{n}{N_A}, \quad \nu(F) = \frac{v(FE_s)}{v_s}. \tag{9}$$

Inserting this in Eqs. (1) and (3)–(8), we obtain

$$\epsilon\left(\frac{\partial F}{\partial s} + \delta\frac{\partial \eta}{\partial y}\right) = j(t) - \eta\nu(F), \tag{10}$$

$$\epsilon\frac{\partial F}{\partial y} = p - 1 - \eta, \tag{11}$$

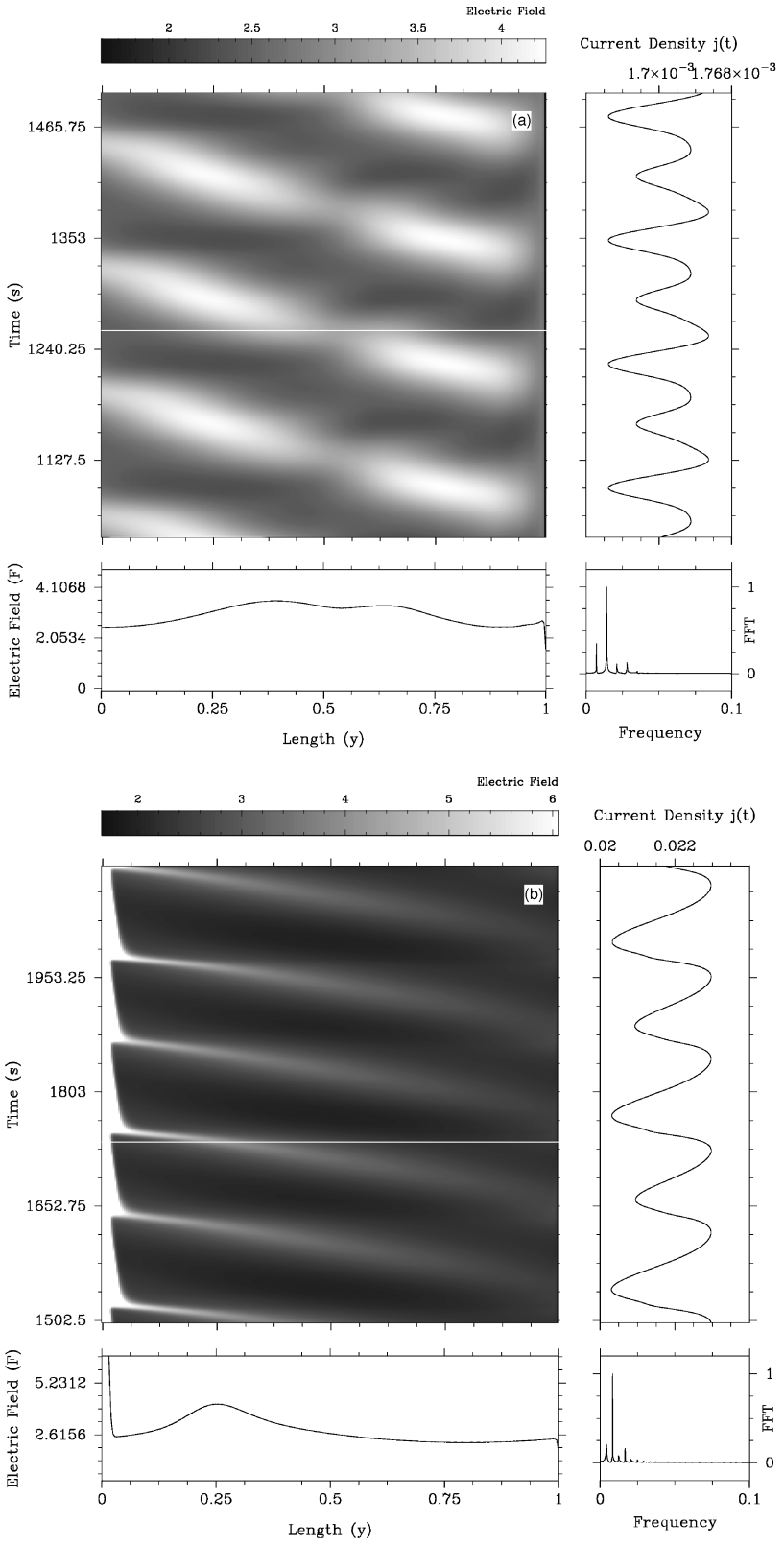

FIG. 2. Numerical simulations for values of the current and the oscillation frequency corresponding to points (a) A, (b) B, (c) C, and (d) D in Fig. 1. All other parameters correspond exactly to those proposed in Ref. 1 (see text). Each figure contains four graphics in dimensionless variables: a spatiotemporal density plot of the electric field, $F(y,s)$ (density scale on the upper right part), a plot of the current density $j(s)$ (upper left), the power spectra of the $j(s)$ signal in arbitrary units (lower right), and the electric field as a function of y for the fixed time marked with a white horizontal line in the $F(y,s)$ density plot (lower left).

$$\frac{\partial p}{\partial s} = i_0[1 + m\ \cos(ky + ws)](1 - \alpha p) - \beta \eta p, \tag{12}$$

$$\int_0^1 F\, dy = \phi. \tag{13}$$

Here we have defined the following nondimensional parameters [we assume constant diffusivity, $D(F) = D$]:

$$\epsilon = \frac{\epsilon_s E_s}{q N_A L}, \quad \phi = \frac{1}{E_s L} V, \quad \delta = \frac{q D N_A}{v_s \epsilon_s E_s}, \quad \beta = \frac{\epsilon_s E_s}{\epsilon v_s q} \gamma,$$

$$\alpha = \frac{N_A}{N_D}, \quad i_0 = \frac{S \epsilon_s E_s N_D}{\epsilon v_s q N_A^2} I_0, \quad w = \frac{\epsilon_s E_s}{\epsilon v_s q N_A} \Omega,$$

$$k = \frac{\epsilon_s E_s}{\epsilon q N_A} K. \tag{14}$$

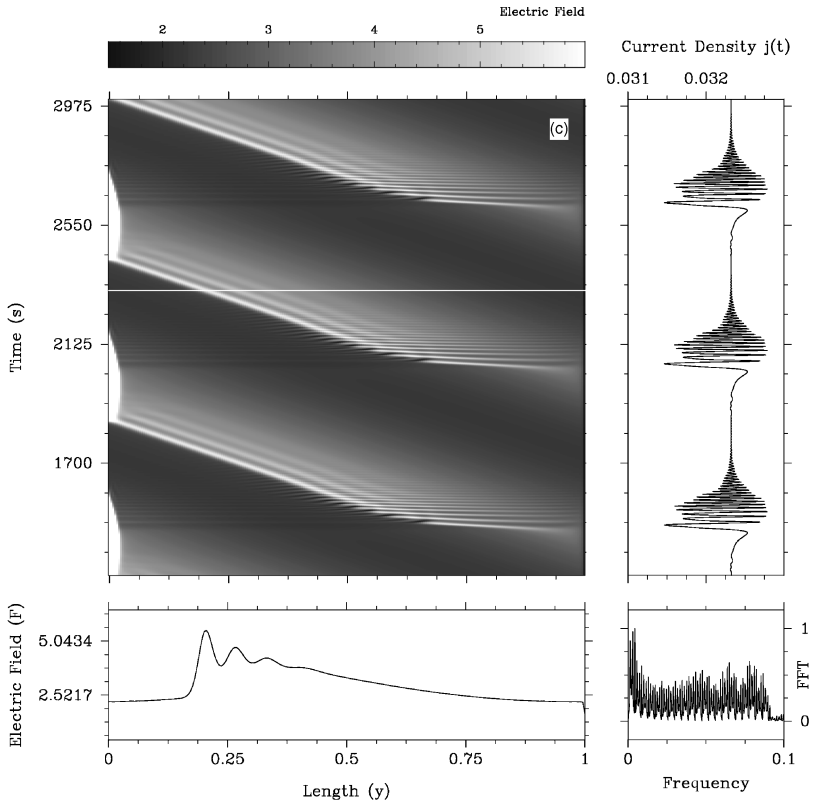

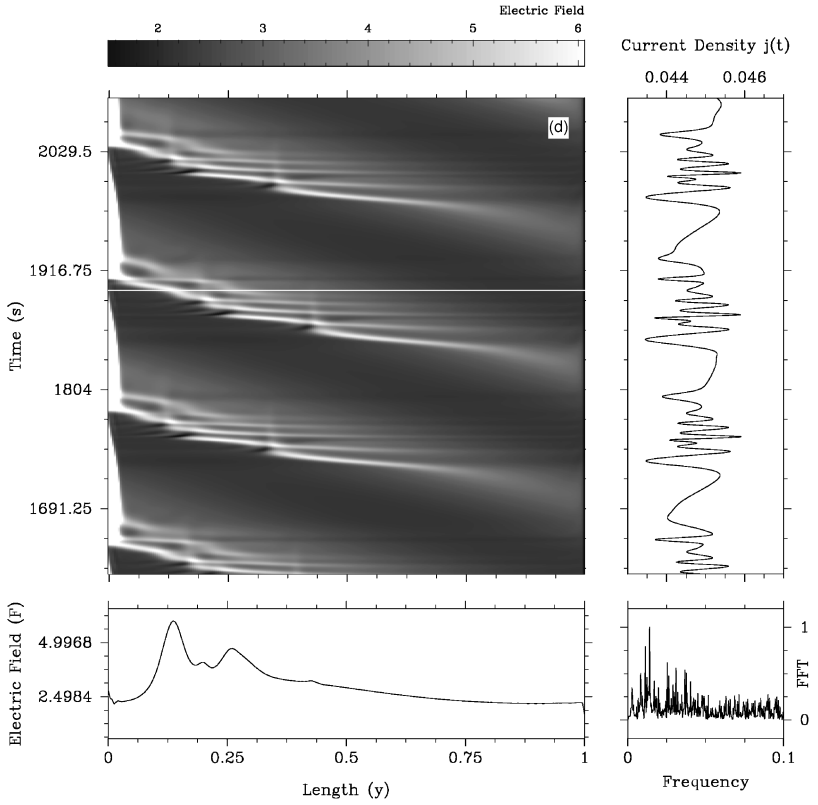

FIG. 2. (*Continued*).

III. RESULTS

We have solved Eqs. (10)–(13) numerically for different values of the parameters w and i_0, keeping fixed $\epsilon = 4.138\times10^{-4}$, $m=0.1$, $\rho=1.8$, $k=2\pi$, $\delta=0.05$, $\alpha=0.01$, $\beta=3.5294$, and $\phi=3$. These numerical values correspond to those used by SCA.[1] We were particularly interested in testing a central piece of SCA's analysis, namely their particular use of Kroemer's *NL* criterion, their Eq. (20). Prompted by SCA's suggestion that the length in Kroemer's criterion may be the distance between multiple domains, we combine their Eq. (20) with their Eq. (17) for the electron density n_1, and use $l=L/N$, where l is the distance between

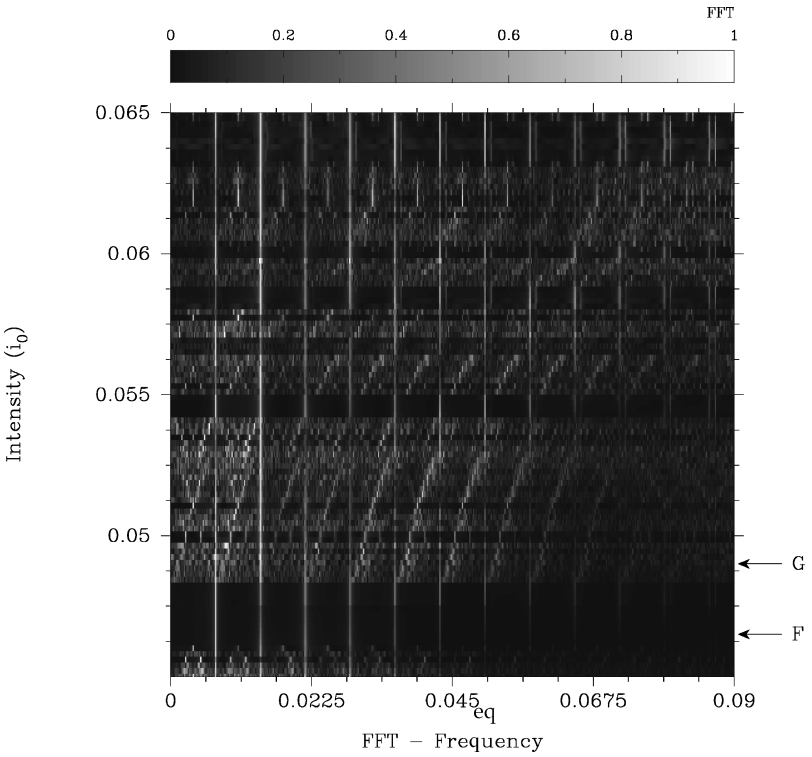

FIG. 3. Fourier power spectra of $j(t)$ for $w=0.05$ and diferent values of i_0 in the range $0.045-0.065$ (line E of Fig. 1). Each FFT is represented by a narrow horizontal band with gray scaled frecuency mode amplitudes: white (large) and black (small), in arbritary units. The arrows correspond to the simulations of a periodic signal (F) and a chaotic one (G) carried out in Fig. 4.

adjacent domains. Then we obtain a formula for the maximum number (N) of high-field domains which may coexist:

$$N<N_0\equiv\frac{195.565}{1+\frac{10^{11}}{I_0}-100\left(\frac{\Omega}{I_0}\right)^2}. \tag{15}$$

We have used SCA's numerical values (I_0 and Ω are measured in W m^{-2} and Hz, respectively). Figure 1 depicts the level curves $\Omega(I_0)$, which are obtained when N_0 takes on different integer values. If SCA's theory holds, $N=i$ between the level curves $N_0=i-1$ and $N_0=i$. However, we observed Gunn domains (Fig. 2, A) where Segev *et al.*'s theory predicts they should not be (point A in Fig. 1). Points C and D in Fig. 1 would correspond to a coexistence of $N=2$ and $N=3$ domains, respectively, but we find four domains and a periodic response (Fig. 2, C) and a quasichaotic response (Fig. 2, D), respectively. Finally, at point B corresponding to the conditions proposed by SCA to illustrate their theory, one domain is created during each oscillation period (Fig. 2, B). In fact, the response of the system is very complex and within each of those zones in the $\Omega(I_0)$ plane, where a constant number of high-field domains is predicted, it is possible to find all kinds of behavior: periodic with a single frequency, periodic with a high number of frequencies, and chaotic.

The discrepancy between the computed and predicted response should not be surprising. In fact, the Gunn effect is a periodic oscillation of the current ($\propto J_{\text{total}}$) in a dc voltage biased semiconductor presenting negative differential velocity. It is due to periodic shedding and motion of charge dipole waves (high field domains) at a boundary or a nucleation site. It is intrinsically nonlinear[3–8] so that the relevance of linear approximations such as those used in Ref. 1 is questionable. We think that Kroemer's NL criterion implies that for a given model (equations, bias, boundary, and initial conditions) it can be proved that no oscillatory instability is possible unless the NL product (where L is semiconductor length and N is doping density) is above a certain number. For Kroemer's model of the Gunn effect in n-GaAs under dc voltage bias, see Fig. 3 of Ref. 9. An analytical estimate (probably not a very precise one) could be obtained by adapting to the Kroemer model the arguments in the Appendix of Ref. 10. This said, SCA have used a particular version of the NL criterion in which N is an electron density and L is either the semiconductor length (one domain) or the distance between domains (multiple domains). It is not surprising that this usage produces results that are not quantitatively correct. Furthermore, the Gunn effect is due to the instability of the ground state and the effect of light is only to trigger this instability. Thus, very small perturbations of light instensity can result in large density perturbations, in contradiction with the linear relationship between the intensity modulation and the electron density perturbation derived by SCA. This has been confirmed by numerical simulations that show the existence of a Gunn effect for very small light intensities.

It is interesting to compare the response of the system in points C and D of Fig. 1. We observe that the dimensionless current density, $j(t)$, in case C is periodic (Fig. 2) although it contains a large number of frequencies, as can be seen in the FFT spectrum shown in the lower right of the figure. Instead, the response in case D is not periodic and the FFT spectrum appears chaotic. The difference between these two cases can be understood by looking at the electric field profiles as a function of time. In case C, there are several waves that originate at the injecting contact (right contact) and propagate towards the receiving contact. Neither of these waves overtakes the previous one and this leads to a smooth, periodic response. In case D, however, a wave originates at the injecting contact and propagates through the sample.

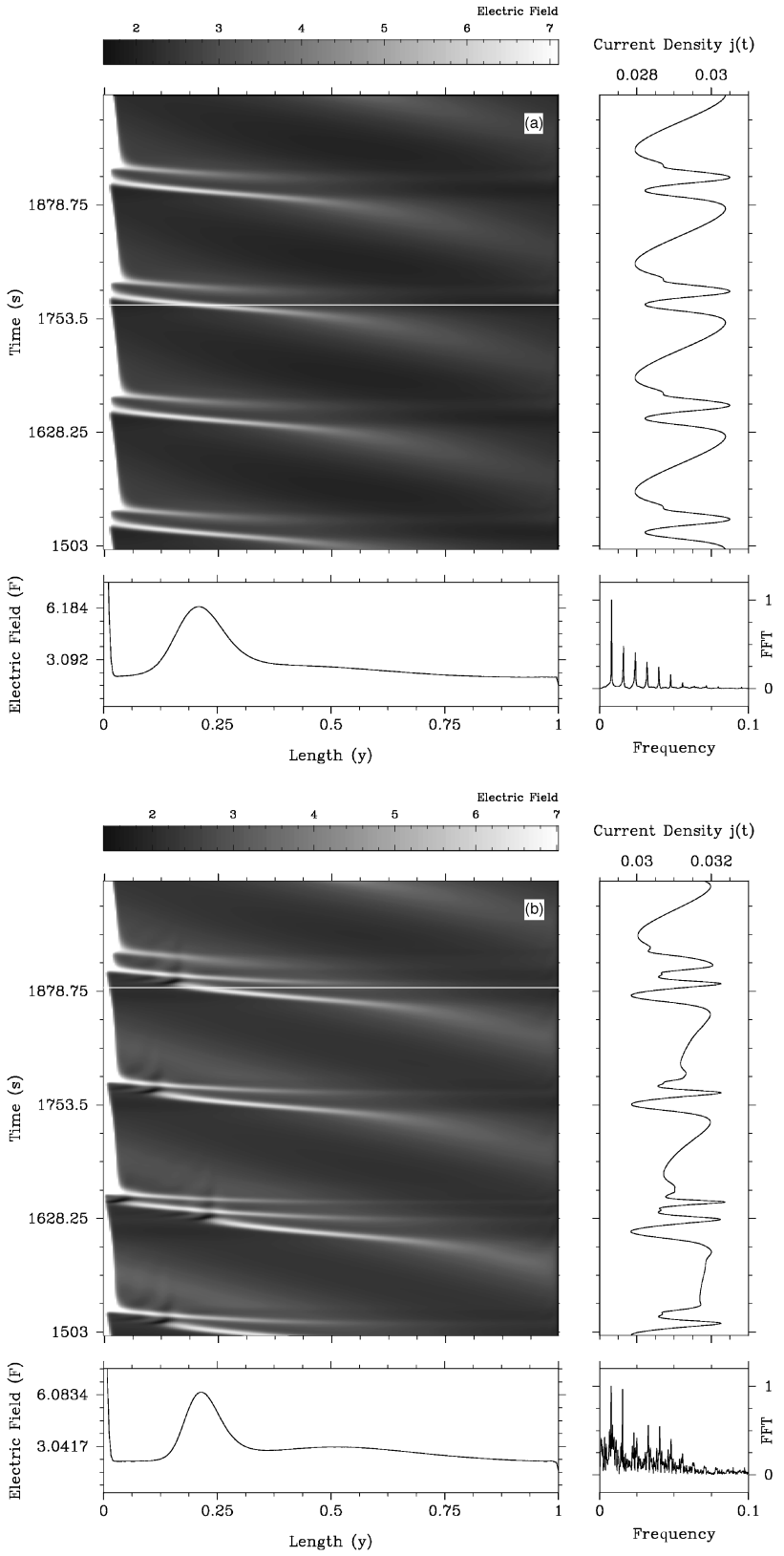

FIG. 4. Numerical simulations for the (a) point F and (b) point G in Fig. 3. The layout of the graphics is the same as in Fig. 2.

Later, a new wave is injected that moves faster than the previous one, and that overtakes it before reaching the receiving contact. The interaction between waves inside the sample leads to a complex response that may become chaotic.

To understand the transition between the periodic and chaotic solutions we carried out numerical simulations for a fixed value of Ω and varying the intensity I_0 within a certain small range corresponding to line E in Fig. 1. The results of these simulations are summarized in Fig. 3, which shows the intensity of each mode of the FFT spectrum as a function of I_0. Notice that there is a frequency, which is very close to the excitation frequency Ω, that appears for all values of I_0. Also, all integer multiples of this frequency are present in the

current density history. It can also be observed that there is a sharp transition between a periodic solution and a chaotic one. Figure 4 shows the current density history and field profiles for case F in the periodic region, and for case G inside the chaotic region.

The bias condition imposes a conservation of area in the electric field profile $E(z)$ for all time. Thus, the size of a traveling wave must decrease when a new wave is generated in the injecting contact (right contact). If the new wave grows fast enough, the old wave must disappear to keep the area constant. In both cases, see F and G in Fig. 4, several waves are born at the injecting contact and propagate towards the receiving contact during a period. In case F, all the waves reach the left contact and this leads to a periodic response in the density current. As the intensity I_0 increases, the wave formation velocity increases until a critical value above which the waves that propagate through the sample disappear before reaching the receiving contact. This produces a complex behavior with different patterns of formation-disappearance of waves. Larger values of I_0 result in chaotic responses such as that shown in case G as an example.

It is also interesting to observe that within the chaotic region there are windows in which the response again becomes periodic, with frecuency given by the fundamental frequency divided by 2, 3, or 4. In these specific ranges of I_0, the interaction between waves inside the sample produces a simple pattern with a periodic sequence.

IV. CONCLUSIONS

We have thus found that high field domains could indeed be triggered by phase-locked interference fringes, as suggested by SCA. However, a literal use of their version of Kroemer's NL criterion does not often agree with numerical simulations of the model for the photorefractive Gunn effect. In addition, we have found very interesting examples of natural and driven (sinusoidal interference pattern of intensity I) chaos when appropriate parameter values are used. In the regime for which the high field domains carry a large fraction of the bias, an asymptotic theory of the Gunn effect[5–8] can be extended and applied to the photorefractive model, and used to interpret and predict the results of the numerical simulations with greater accuracy than SCA's linearized approach. These results will be presented elsewhere.

[1] M. Segev, B. Collings, and D. Abraham, Phys. Rev. Lett. **76**, 3798 (1996).
[2] L. Subacius, V. Gruzinskis, E. Starikov, P. Shiktorov, and K. Jarasiunas, Phys. Rev. B **55**, 12 844 (1997).
[3] S. M. Sze, *Physics of Semiconductor Devices*, 2nd ed. (Wiley, New York, 1981).
[4] M. P. Shaw, H. L. Grubin, and P. R. Solomon, *The Gunn-Hilsum Effect* (Academic Press, New York, 1979).
[5] F. J. Higuera and L. L. Bonilla, Physica D **57**, 161 (1992).
[6] L. L. Bonilla, P. J. Hernando, M. Kindelan, M. A. Herrero, and J. J. L. Velázquez, Physica D **108**, 168 (1997).
[7] L. L. Bonilla, I. R. Cantalapiedra, G. Gomila, and J. M. Rubí, Phys. Rev. E **56**, 1500 (1997).
[8] L. L. Bonilla and I. R. Cantalapiedra, Phys. Rev. E **56**, 3628 (1997).
[9] L. L. Bonilla, F. J. Higuera, and S. Venakides, SIAM (Soc. Ind. Appl. Math.) J. Appl. Math. **54**, 1521 (1994).
[10] A. Wacker, M. Moscoso, M. Kindelan, and L. L. Bonilla, Phys. Rev. B **55**, 2466 (1997).